Physics Letters B 728 (2014) 308–313

Contents lists available at ScienceDirect

Physics Letters B

www.elsevier.com/locate/physletb

Di-Higgs final states augMT2ed – Selecting *hh* events at the high luminosity LHC

Alan J. Barr [a], Matthew J. Dolan [b], Christoph Englert [c,*], Michael Spannowsky [b]

[a] Denys Wilkinson Building, Department of Physics, Keble Road, Oxford, OX1 3RH, United Kingdom
[b] Institute for Particle Physics Phenomenology, Department of Physics, Durham University, DH1 3LE, United Kingdom
[c] SUPA, School of Physics and Astronomy, University of Glasgow, Glasgow, G12 8QQ, United Kingdom

ARTICLE INFO

Article history:
Received 1 October 2013
Received in revised form 28 November 2013
Accepted 2 December 2013
Available online 6 December 2013
Editor: A. Ringwald

ABSTRACT

Higgs boson self-interactions can be investigated via di-Higgs ($pp \to hh + X$) production at the LHC. With a small $\mathcal{O}(30)$ fb Standard Model production cross section, and a large $t\bar{t}$ background, this measurement has been considered challenging, even at a luminosity-upgraded LHC. We demonstrate that by using simple kinematic bounding variables, of the sort already employed in existing LHC searches, the dominant $t\bar{t}$ background can be largely eliminated. Simulations of the signal and the dominant background demonstrate the prospect for measurement of the di-Higgs production cross section at the 30% level using 3 ab^{-1} of integrated luminosity at a high luminosity LHC. This corresponds to a Higgs self-coupling determination with 60% accuracy in the $b\bar{b}\tau^+\tau^-$ mode, with potential for further improvements from e.g. subjet technologies and from additional di-Higgs decay channels.

1. Introduction

After a particle consistent with the Standard Model (SM) Higgs boson has been discovered at the LHC [1,2], we have the final irrefutable experimental evidence of the realisation of a Higgs mechanism in nature [3–6]. This discovery alone, however, does not provide us the full details of this symmetry breaking sector. In particular, we do not have any additional information other than the existence of a (local) symmetry-breaking minimum and the Higgs potential's curvature at this point in field space. These are rather generic properties of symmetry breaking potentials which can easily be reconciled with more complex scenarios of electroweak symmetry breaking. These typically exhibit a significantly different form of the Higgs self-interaction from the SM,[1] and to obtain a better understanding of how electroweak symmetry breaking comes about, we need to find a way to discriminate between these different realisations.

The only direct way to provide a satisfying discrimination between the SM symmetry breaking sector and more complicated realisations is probing higher order terms of the Higgs potential directly. In practice this means studying multi-Higgs final states and inferring the relevant couplings from data. The size of the cross sections at the LHC and future colliders effectively limits such a program to the investigation of the trilinear Higgs coupling λ [8]. In the SM, λ is a function of the Higgs mass m_h and the quartic Higgs interaction η,

$$V(H^\dagger H) = \mu^2 H^\dagger H + \eta (H^\dagger H)^2 \to \frac{1}{2} m_h^2 h^2 + \sqrt{\frac{\eta}{2}} m_h h^3 + \frac{\eta}{4} h^4,$$

where we have expanded the potential around the non-zero Higgs vacuum expectation value in unitary gauge in the second line which yields $\lambda_{\rm SM} = m_h \sqrt{\eta/2}$.

The effort of phenomenologically reconstructing the trilinear Higgs coupling is based on di-Higgs production $pp \to hh + X$ [9–14] and dates back more than a decade [15–18], but in the light of the recent Higgs discovery it has gained new momentum [14,19–29]. Probably the most promising approach to infer the trilinear coupling which has been proposed so far is via $hh \to b\bar{b}\tau^+\tau^-$. The hadron-level analysis of Ref. [19] demonstrated that bounds could be set on *hh* production at the LHC by using high-$p_{\rm T}$ final states and boosted techniques [30,31]. Inclusive analyses on the other hand are limited by a large $t\bar{t}$ background [16]. The analysis of Ref. [19] was conservative in the sense that it did not employ

* Corresponding author.
E-mail addresses: a.barr@physics.ox.ac.uk (A.J. Barr), m.j.dolan@durham.ac.uk (M.J. Dolan), christoph.englert@glasgow.ac.uk (C. Englert), michael.spannowsky@durham.ac.uk (M. Spannowsky).

[1] For example in scenarios in which the electroweak symmetry is broken radiatively, we typically encounter Coleman–Weinberg type potentials [7] which exhibit an infinite power series in the Higgs field with model-dependent expansion coefficients.

0370-2693
http://dx.doi.org/10.1016/j.physletb.2013.12.011

selection criteria based on missing transverse momentum, which have the potential to reduce the most challenging $t\bar{t}$ backgrounds.

In the present Letter we complement the analysis of Ref. [19] along these lines and also address the question of the extent to which a successful analysis of the di-Higgs final state will depend on the overall Higgs boost. We concentrate on the $bb\tau^+\tau^-$ mode,

$$pp \to hh + X \to (b + \bar{b}) + \left(\tau^+ + \tau^-\right) + X, \tag{1}$$

for which the $t\bar{t}$ background process

$$\begin{aligned} pp \to t\bar{t} + X &\to \left(b + W^+\right) + \left(\bar{b} + W^-\right) + X \\ &\to \left(b + \tau^+ + \nu_\tau\right) + \left(\bar{b} + \tau^- + \bar{\nu}_\tau\right) + X \end{aligned} \tag{2}$$

dominates. We use kinematical properties of the decay of Eq. (2) to greatly reduce the $t\bar{t}$ background.

While we focus on the $bb\tau^+\tau^-$ mode in this Letter, we note that variants of the technique would be applicable to a broader range of di-Higgs decay modes, particularly others also involving the $h \to b\bar{b}$ and $h \to W^+W^-$ decays, which have the largest branching ratios for a 125 GeV Standard Model Higgs boson.

2. Kinematic bounding variables

The dominant $t\bar{t}$ background can be reduced by using the m_{T2} variable, sometimes called the 'stransverse mass' [32,33]. This mass-bound variable was designed for the case where a pair of equal-mass particles decay,

$$A \to B + C,$$
$$A' \to B' + C',$$

and where one daughter from each parent, B or B', is a visible particle, and the other, C or C' is not observed. Since the Cs are invisible their individual four-momenta are not known. However the vector sum $\mathbf{p}_{\mathrm{T}}^{\Sigma}$ of the transverse momentum components of C and C' can be determined from momentum conservation in the plane perpendicular to the beam.

For any given event m_{T2} is defined to be the maximal possible mass of the parent particle A consistent with the constraints; that is m_{T2} provides the greatest lower bound on $m_A = m_{A'}$ given the experimental observables [34].

In the context of the di-Higgs decay (1) the dominant background process (2) satisfies the assumptions under which m_{T2} is useful: the dileptonic (di-tau) $t\bar{t}$ background involves the pair-production of identical-mass parents; and each of which decays to a final state which contains visible particles (the b jets, and visible τ decay products) and invisible particles (the neutrinos both from the W decays and from the leptonic or hadronic τ decays). We can therefore build a kinematical variable from the observed final state particles which is bounded above by the top quark mass for the $t\bar{t}$ background, but remains unbounded above for the di-Higgs signal process.

The m_{T2} variable can be explicitly constructed [32] as

$$\begin{aligned} &m_{\mathrm{T2}}\left(m_B, m_{B'}, \mathbf{b}_{\mathrm{T}}, \mathbf{b}'_{\mathrm{T}}, \mathbf{p}_{\mathrm{T}}^{\Sigma}, m_C, m_{C'}\right) \\ &\quad\equiv \min_{\mathbf{c}_{\mathrm{T}} + \mathbf{c}'_{\mathrm{T}} = \mathbf{p}_{\mathrm{T}}^{\Sigma}} \left\{\max\left(m_{\mathrm{T}}, m'_{\mathrm{T}}\right)\right\}, \end{aligned} \tag{3}$$

where m_{T} is the transverse mass constructed from m_B, m_C, $\mathbf{b}_{\mathrm{T}}$ and $\mathbf{c}_{\mathrm{T}}$, while m'_{T} is the transverse mass constructed from $m_{B'}$, $m_{C'}$, $\mathbf{b}'_{\mathrm{T}}$ and $\mathbf{c}'_{\mathrm{T}}$, and where the minimisation is over all hypothesised transverse momenta $\mathbf{c}_{\mathrm{T}}$ and $\mathbf{c}'_{\mathrm{T}}$ for the invisible particles which sum to the constraint $\mathbf{p}_{\mathrm{T}}^{\Sigma}$, which is usually the observed missing transverse momentum $\vec{\not{p}}_{\mathrm{T}}$. The transverse mass m_{T} is itself defined by

$$m_{\mathrm{T}}^2(\mathbf{b}_{\mathrm{T}}, \mathbf{c}_{\mathrm{T}}, m_b, m_c) \equiv m_b^2 + m_c^2 + 2(e_b e_c - \mathbf{b}_{\mathrm{T}} \cdot \mathbf{c}_{\mathrm{T}}),$$

where the 'transverse energy' e for each particle is defined by

$$e^2 = m^2 + \mathbf{p}_{\mathrm{T}}^2.$$

Variants[2] of m_{T2} address cases where some or all of the A, B, A' or B' particles are composed of four-vector sums. Such variants are designed for more complicated n-body decays with $n > 2$ or for the case of sequential decays with on-shell intermediates. While these mass-bounding variables were originally proposed to gain sensitivity to the masses of new particles at hadron colliders, they have also proved effective in searches [37–41].

For the $hh \to bb\tau^+\tau^-$ case, an appropriate variable is constructed as follows. The b jets resulting from each of the two top quark decays enter (3) as the visible particles B and B'. The components C and C' in (3) which form the transverse momentum constraint should then be the sum of the decay products of the W bosons. The appropriate vector sum $\mathbf{p}_{\mathrm{T}}^{\Sigma}$ for the constraint in (3) contains both visible and invisible components,

$$\begin{aligned} \mathbf{p}_{\mathrm{T}}^{\Sigma} &\equiv \vec{\not{p}}_{\mathrm{T}} + \mathbf{p}_{\mathrm{T}}^{\mathrm{vis}}(\tau) + \mathbf{p}_{\mathrm{T}}^{\mathrm{vis}}\left(\tau'\right) \\ &= \mathbf{p}_{\mathrm{T}}(W) + \mathbf{p}_{\mathrm{T}}\left(W'\right), \end{aligned} \tag{4}$$

where the first line sums the missing transverse momentum $\vec{\not{p}}_{\mathrm{T}}$ (from all neutrinos from the leptonic W decays, including subsequent leptonic or hadronic τ decays), and the visible transverse momentum from each of the two reconstructed τ candidates.

The resulting variable

$$m_{\mathrm{T2}}\left(m_b, m'_b, \mathbf{b}_{\mathrm{T}}, \mathbf{b}'_{\mathrm{T}}, \mathbf{p}_{\mathrm{T}}^{\Sigma}, m^{\mathrm{vis}}(\tau), m^{\mathrm{vis}}\left(\tau'\right)\right) \tag{5}$$

is by construction bounded above by m_t for the $t\bar{t}$ background process (in the narrow width approximation, and in the absence of detector resolution effects). By contrast, for the hh signal the m_{T2} distribution can reach very large values, in principle up to $\sqrt{s}/2$.

3. Elements of the analysis

3.1. Detector simulation

We model the effects of detector resolution and efficiency using a custom detector simulation based closely on the ATLAS 'Kraków' parameterisation [42]. The parameters employed provide conservative estimates of the ATLAS detector performance for the phase-II high luminosity LHC machine (HL-LHC), which is expected to deliver an integrated luminosity of 3 ab^{-1} to each of the two general-purpose experiments. In particular we model pile-up (at $\mu = 80$, where μ is the mean number of pile-up events per bunch crossing) and $\sum E_{\mathrm{T}}$ dependent resolutions for jets and for $\not{p}_{\mathrm{T}}$.

Jets are reconstructed with the anti-k_t jet clustering algorithm [43,44] with radius parameter 0.6. Tau lepton reconstruction efficiencies and fake rates are included, based on Ref. [42], as are jet resolutions, and b-jet efficiencies and fake rates.

3.2. Event generation

To generate the signal and background events we closely follow Ref. [19] (details of the comparison of the signal Monte Carlo that underlies this study and comparisons against earlier results can be found therein). Signal events $p(g)p(g) \to hh + X$ (which dominate the inclusive hh cross section) are generated with a combination of the VBFNLO [45] and FeynArts/FormCalc/LoopTools [46,47] frameworks. We generate events in the Les Houches standard [48] which

[2] See Ref. [35] for a recent review, and Ref. [36] for examples and categorisation.

Table 1
Cross sections for the hh signal and for the dominant backgrounds after various selection criteria have been applied. The $b\bar{b}W^+W^-$ column considers only the decay of W bosons to τ leptons, and already includes the corresponding branching ratios. The final column shows the signal-to-background ratio. The numbers in brackets follow from a more conservative $\tau\tau$ mass reconstruction, described in the text. The last rows correspond to exemplary cuts $p_{\mathrm{T},b\bar{b}} \geqslant 175$ GeV followed by $m_{\mathrm{T2}} \geqslant 125$ GeV.

Cross section [fb]	Signal	Backgrounds			S/B
	hh	$b\bar{b}W^+W^-$	$b\bar{b}\tau^+\tau^-$	$b\bar{b}\tau^+\tau^-$ ew.	
Before cuts	13.89	10792	2212	82.3	1.06×10^{-3}
After trigger	1.09	1966	372	15.0	0.463×10^{-3}
After event selection	0.248	383.0	43.7	2.08	0.578×10^{-3}
After $m(\tau^+\tau^-)$ cut	0.164 [0.128]	107.7 [107.4]	4.62 [16.0]	0.316 [0.789]	1.46×10^{-3} [1.02×10^{-3}]
After $m(b\bar{b})$ cut	0.118 [0.093]	28.7 [29.1]	0.973 [4.03]	0.062 [0.351]	3.98×10^{-3} [2.79×10^{-3}]
After $p_{\mathrm{T},b\bar{b}}$ cut	0.055 [0.041]	0.475 [0.480]	0.037 [0.247]	0.013 [0.079]	0.105 [0.050]
After m_{T2} cut	0.047 [0.034]	0.147 [0.194]	0.029 [0.204]	0.012 [0.074]	0.250 [0.072]

we pass to Herwig++ [49] for showering and hadronisation of the selected $h \to b\bar{b}, \tau^+\tau^-$ final states. We use a flat NLO QCD factor to account for higher order perturbative corrections by effectively normalising to an inclusive cross section of $\sigma = 33.89$ fb [22,50]. Recent calculations show this may be increased by a further 20% by NNLO contributions [13,14,51], which we do not include here.

The QCD and electroweak $b\bar{b}\tau^+\tau^-$ backgrounds are generated with Sherpa [52] and the $t\bar{t}$ background of Eq. (2) is generated with MadEvent 5 [53]. The $b\bar{b}W^+W^-$ NLO cross sections have been computed in Ref. [54] (we use $K \simeq 1.5$ and specify $W \to \tau\nu_\tau$ in Herwig++ during showering and hadronisation to increase the efficiency for the cut selection), for the mixed QCD/electroweak and the purely electroweak contributions we use the corrections to $Zb\bar{b}$ ($K \simeq 1.4$) and ZZ ($K \simeq 1.6$) production using Mcfm [55–57].

3.3. Event selection

Events are assumed to pass the trigger if there are at least two τs with visible $p_{\mathrm{T}} > 40$ GeV or at least one τ with visible $p_{\mathrm{T}} > 60$ GeV. Both leptonic and hadronic decays of τs are included. Selected events are required to have exactly two reconstructed τs (leptonic or hadronic) and exactly two reconstructed and b-tagged jets.

The reconstruction of the di-tau mass is important in discriminating the $h \to \tau^+\tau^-$ from the $Z \to \tau^+\tau^-$ background. The LHC experiments typically employ sophisticated mass-reconstruction methods which include kinematic constraints but also likelihood functions or multi-variate techniques trained to mitigate against detector resolution [58,59]. We use a simpler, purely kinematic reconstruction of the di-tau mass, which is not expected to perform as well as the techniques used by the experiments in the presence of detector smearing. To estimate the systematic impact of the τ reconstruction on $h \to \tau\tau$ selection, we perform the same $m^{>}_{\tau\tau}$ reconstruction with and without simulation of the $\not{p}_{\mathrm{T}}$ resolution. The more sophisticated techniques used by the experiments which mitigate against detector resolution can be expected to lie between our two estimates.

In each case we construct a $\tau^+\tau^-$ invariant mass bound $m^{>}_{\tau\tau}$ using the greatest lower bound $m^{\text{Higgs-bound}}_{\tau\tau}$ on m_h given the visible momenta, $\not{p}_{\mathrm{T}}$ and m_τ constraints [60]. When detector smearing leads to events where $m^{\text{Higgs-bound}}_{\tau\tau}$ does not exist, the τ mass constraints are dropped, and the resulting transverse mass m_{T} is used as the greatest lower bound $m^{>}_{\tau\tau}$ on m_h.

In each case we require that $m^{>}_{\tau\tau}$ lie within a 50 GeV window. In the analysis without $\not{p}_{\mathrm{T}}$ smearing we choose 100 GeV $< m_{\tau\tau} <$ 150 GeV, while we select 80 GeV $< m_{\tau\tau} <$ 130 GeV when smearing is included. This shift in the di-tau mass window is required to capture all the signal, since the smearing alters the $\not{p}_{\mathrm{T}}$ distribution and hence the τ reconstruction. Also note that in this case $Z \to \tau^+\tau^-$ is a large contamination of the signal region defined by the invariant mass windows. By calibrating the Higgs mass reconstruction from $h \to \tau^+\tau^-$ as already presently performed in the $Z \to \tau^+\tau^-$ case [61,62], this contamination could be reduced.

The $b\bar{b}$ invariant mass is calculated from the four-vector sum of the two b-tagged jets. Events are selected if they satisfy 100 GeV $< m_{bb} <$ 150 GeV.

4. Results

The numbers of events passing each of the selection criteria are tabulated in Table 1. We find that the transverse momentum and m_{T2} observables are necessary for background suppression, and, hence, for a potentially successful measurement of the di-Higgs final state in a hadronically busy environment. The normalised m_{T2} and $p_{\mathrm{T},b\bar{b}}$ distributions after the selection shown in Table 1 are plotted in Fig. 1. It can be seen that each of the two variables offers good signal versus background discrimination at the large integrated luminosities anticipated at the high luminosity LHC. We also observe that m_{T2} and $p_{\mathrm{T},b\bar{b}}$ encode complementary information about the event kinematics such that they can be combined towards an optimised search strategy.

We find it is straightforward to obtain signal-to-background (S/B) ratios of $\sim$1/5 while retaining an acceptably large signal cross section. These ratios are re-expressed in Fig. 2 which depicts the luminosity contours that are necessary to claim a 5σ discovery of di-Higgs production on the basis of a simple 'cut and count' experiment that makes the rectangular cut requirements that both $p_{\mathrm{T},b\bar{b}} > p_{\mathrm{T},b\bar{b}}(\text{cut})$ and $m_{\mathrm{T2}} > m_{\mathrm{T2}}(\text{cut})$. Both axes stop at rather low values of $(p_{\mathrm{T},b\bar{b}}, m_{\mathrm{T2}})$ since a tighter selection would be dependent on the tail of the $t\bar{t}$ distribution where $S/\sqrt{B}$ does not provide an appropriate indicator of sensitivity. We find that the HL-LHC has good sensitivity to the hh production at high luminosity. For an example selection we obtain a cross section measurement in the 30% range (including the statistical background uncertainty).

The sensitivity to the Higgs trilinear coupling follows from destructive interference with other SM diagrams (see Ref. [19]), such that

$$\lambda \gtrless \lambda_{\mathrm{SM}} \quad \Longrightarrow \quad \sigma(hh) \lessgtr \sigma(hh)_{\mathrm{SM}}. \tag{6}$$

Using the full parton-level $p(g)p(g) \to hh + X$ calculation [19] we find that the quoted 30% cross section uncertainty translates into 60% level sensitivity to the Higgs trilinear coupling in the part of the $p_{\mathrm{T},b\bar{b}}$ distribution which is relevant for this analysis, $p_{\mathrm{T},b\bar{b}} \gtrsim 180$ GeV.

As an alternative to a 'cut and count' analysis we construct a two-dimensional likelihood from $(m_{\mathrm{T2}}, p_{\mathrm{T},b\bar{b}})$ to obtain an estimate of the maximal sensitivity that is encoded in these observables, including their correlation [63]. Figs. 1 and 2 show that the best sensitivity will result from energetic events either with large

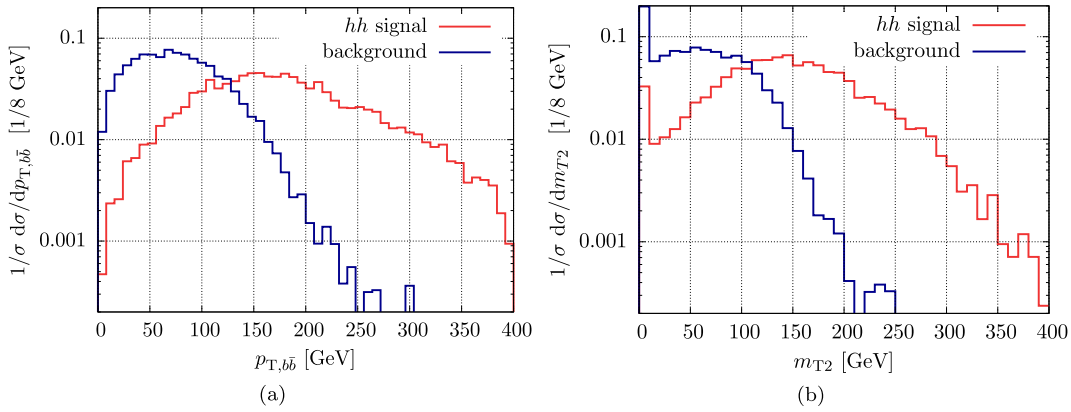

Fig. 1. Transverse momentum distribution of the reconstructed Higgs (i.e. the $b\bar{b}$ pair) and the m_{T2} distribution after the analysis steps described in the text have been carried out (see also Table 1) but before cuts on either m_{T2} or $p_{\mathrm{T},b\bar{b}}$ have been applied.

m_{T2} or large $p_{\mathrm{T},b\bar{b}}$ or both. Using the likelihood method we find fractional uncertainty in the cross section of

$$\left[\sigma/\sigma(hh)_{\mathrm{SM}}\right]_{\mathrm{excl}} \simeq 0.37\ [1.00]$$
$$\text{for } 3\ \mathrm{ab}^{-1} \text{ at } 95\% \text{ confidence level} \qquad (7)$$

using the CL(s) method [64]. The number in brackets refers to the more conservative τ pair resolution described above.

The sensitivity to the $pp \to hh + X$ cross section as captured in Eq. (7) can be rephrased into an expected upper 95% CL bound on the Higgs self-interaction in the $b\bar{b}\tau^+\tau^-$ channel via Eq. (6). For a background-only hypothesis with no true hh production we would find a limit on the self-coupling of

$$\lambda > \lambda|^{3000/\mathrm{fb}}_{95\%\,\mathrm{CL}} \simeq 3.0\ [1.0] \times \lambda_{\mathrm{SM}},$$

where it should be noted that a 95% CL of $3\lambda_{\mathrm{SM}}$ is more stringent than the case of $1\lambda_{\mathrm{SM}}$ due to the destructive interference Eq. (6) (i.e. the di-Higgs cross section for $\lambda = 3\lambda_{\mathrm{SM}}$ is smaller than for $\lambda = \lambda_{\mathrm{SM}}$ for the imposed cuts).

While the limit might be somewhat degraded by additional systematic uncertainties in background determination, it also has the potential to be improved by using a subjet analysis [19], and/or by using the more sophisticated di-tau mass reconstruction techniques already employed by the LHC experiments.

Let us quickly comment on the implications of this analysis for physics beyond the SM. A measurement of the di-Higgs cross section at the level of Eq. (7) would be sufficient to constrain a wide range of scenarios of electroweak symmetry breaking, such as, e.g., composite-Higgs models and pseudo-dilaton models.

In composite scenarios we expect the presence of additional top partners, a decreased Higgs self-coupling and new interactions that couple the top and top partners to two Higgs fields in an effective field theory approach (see e.g. [65]). We do not only expect a larger total di-Higgs cross section in these models when all effects are properly taken into account [66,67], but also the reconstructed Higgs $p_{\mathrm{T},b\bar{b}}$ distribution becomes skewed towards higher values due to the new interactions and the new top partner energy scales leaving footprints in the gluon fusion loops [21]. Cutting on large values of $p_{\mathrm{T},b\bar{b}}$ and m_{T2} will be much more efficient than for the presented SM-like Higgs coupling variation in these scenarios.

Pseudo-dilaton models can show an even larger increase for energetic events since the Higgs self-interaction becomes momentum-dependent. It is enhanced for large momentum transfers and the triangle contribution can become dominant. Additionally, one also expects the presence of new contributions to the box- and triangle-like $gg \to hh$, $gg \to h^*$ diagrams from the states of the

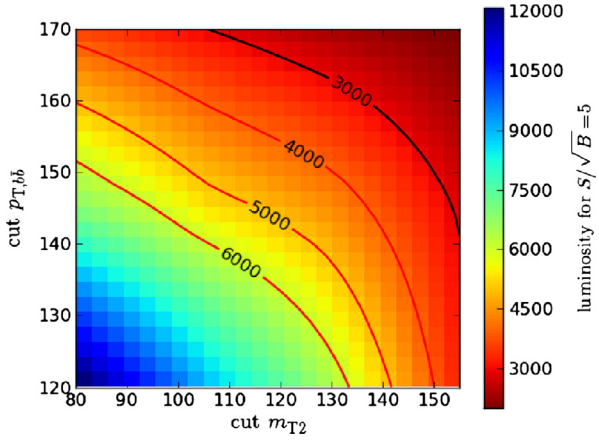

Fig. 2. Luminosity in fb^{-1} required to reach $S/\sqrt{B} = 5$ for di-Higgs production based on simple rectangular cuts on $p_{\mathrm{T},b\bar{b}}$ and m_{T2}. Numbers in red show luminosities that would require a combination of the ATLAS and CMS data sets from a 3 ab^{-1} high luminosity LHC. (For interpretation of the references to color in this figure legend, the reader is referred to the web version of this article.)

conformal sector [68]. The hh cross section can be greatly enhanced even if the single h cross section is compatible with the SM expectation [21].

Since limit setting is based on a statistically resolvable departure from a background null-hypothesis, Eq. (7) implies strong constraints on the above BSM scenarios and any other non-resonant model of new physics with a larger di-Higgs cross section,[3] in the absence of signal-like events. In many of these scenarios, depending on the underlying theory, such a limit needs to be interpreted in the multi-dimensional parameter space of the particular model.

5. Summary and conclusions

Following the discovery of a Higgs boson, one of the top priorities at the LHC is to address the mechanism of electroweak symmetry breaking at a more fundamental level.

In this work we have shown that the 3 ab^{-1} high luminosity LHC will have sensitivity to the Higgs self-coupling in the favoured $b\bar{b}\tau^+\tau^-$ channel using two simple kinematic variables m_{T2} and $p_{\mathrm{T},b\bar{b}}$ each of which independently suppresses the dominant $t\bar{t}$ background.

[3] This also includes off-resonance distributions in resonant models, such as the MSSM.

We have used parameterised detector simulations of the ATLAS detector as expected for a high luminosity environment throughout.

Using a two-dimensional log-likelihood approach, the null hypothesis of $\sigma(hh) = 0$ would constrain the Higgs trilinear coupling to $\lambda \gtrsim 3.0\ [1.0] \times \lambda_{\mathrm{SM}}$ at the 95% confidence level. The number in brackets refers again to the more conservative τ pair mass resolution. An exemplary cross section measurement with 30% precision translates into a measurement of λ at the 60% level.

However further improvements to the presented analysis are possible:

1. Jet substructure techniques allow one to narrow the invariant $b\bar{b}$ mass window [19], thus leading to a larger rejection of the $b\bar{b}W^+W^-$ and $b\bar{b}\tau^+\tau^-$ backgrounds.
2. Calibrated $h \to \tau^+\tau^-$ taggers [61,62] will highly suppress the $b\bar{b}\tau^+\tau^-$ backgrounds and also further reduce the $t\bar{t}$ background.
3. We have used a definition of m_{T2} which does not include any information about the τ lepton momenta other than the sum of their p_{T} in (4). Using calibrated taggers, further kinematic information is available by modifying Eq. (5) through pairing τ and b objects, and exploiting the Jacobian peak of $m_{b\tau}$ in the top decay [69]. One can pair the hardest τ with that particular b jet that yields an $m_{b\tau}$ value that is closer to 140 GeV (the maximum of the Jacobian peak). The leftover b jet is paired with the softer τ, and the following substitutions used in Eq. (5)

$$m_b \to m_{b\tau},$$
$$\mathbf{b}' \to \mathbf{b}' + \boldsymbol{\tau}',$$
$$\mathbf{p}_{\mathrm{T}}^{\Sigma} \to \not{p}_{\mathrm{T}},$$
$$m^{\mathrm{vis}} \to m_{b\tau}^{\mathrm{vis}},$$

where the latter line indicates that the visible τ decay products are included in the invariant visible mass definition.

A combination of such techniques can be used by the LHC experiments to gain improved sensitivity to the Higgs self-coupling – and hence to the nature of electroweak symmetry breaking.

Acknowledgements

This work was supported by the Science and Technology Research Council of the United Kingdom, by Merton College, Oxford, and by the Institute for Particle Physics Phenomenology Associate Scheme. A.J.B. thanks NORDITA and the IPPP for their hospitality during the preparation of this Letter. C.E. thanks the IPPP for hospitality during the time when this work was completed. We thank Margarete Mühlleitner and Michael Spira for interesting discussions during the 2013 Les Houches workshop. Also, we thank Mike Johnson, Peter Richardson, and Ewan Steele for computing support and their patience.

References

[1] G. Aad, et al., ATLAS Collaboration, Phys. Lett. B 716 (2012) 1, arXiv:1207.7214.
[2] S. Chatrchyan, et al., CMS Collaboration, Phys. Lett. B 716 (2012) 30, arXiv:1207.7235.
[3] P.W. Higgs, Phys. Lett. 12 (1964) 132.
[4] P.W. Higgs, Phys. Rev. Lett. 13 (1964) 508.
[5] G. Guralnik, C. Hagen, T. Kibble, Phys. Rev. Lett. 13 (1964) 585.
[6] F. Englert, R. Brout, Phys. Rev. Lett. 13 (1964) 321.
[7] S.R. Coleman, E.J. Weinberg, Phys. Rev. D 7 (1973) 1888.
[8] T. Plehn, M. Rauch, Phys. Rev. D 72 (2005) 053008, arXiv:hep-ph/0507321.
[9] E.N. Glover, J. van der Bij, Nucl. Phys. B 309 (1988) 282.
[10] D.A. Dicus, C. Kao, S.S. Willenbrock, Phys. Lett. B 203 (1988) 457.
[11] T. Plehn, M. Spira, P. Zerwas, Nucl. Phys. B 479 (1996) 46, arXiv:hep-ph/9603205.
[12] A. Djouadi, W. Kilian, M. Muhlleitner, P. Zerwas, Eur. Phys. J. C 10 (1999) 45, arXiv:hep-ph/9904287.
[13] D. de Florian, J. Mazzitelli, Phys. Lett. B 724 (2013) 306, arXiv:1305.5206.
[14] J. Grigo, J. Hoff, K. Melnikov, M. Steinhauser, Nucl. Phys. B 875 (2013) 1, arXiv:1305.7340.
[15] U. Baur, T. Plehn, D.L. Rainwater, Phys. Rev. D 67 (2003) 033003, arXiv:hep-ph/0211224.
[16] U. Baur, T. Plehn, D.L. Rainwater, Phys. Rev. D 68 (2003) 033001, arXiv:hep-ph/0304015.
[17] U. Baur, T. Plehn, D.L. Rainwater, Phys. Rev. D 69 (2004) 053004, arXiv:hep-ph/0310056.
[18] U. Baur, T. Plehn, D.L. Rainwater, Phys. Rev. Lett. 89 (2002) 151801, arXiv:hep-ph/0206024.
[19] M.J. Dolan, C. Englert, M. Spannowsky, J. High Energy Phys. 1210 (2012) 112, arXiv:1206.5001.
[20] A. Papaefstathiou, L.L. Yang, J. Zurita, Phys. Rev. D 87 (2013) 011301, arXiv:1209.1489.
[21] M.J. Dolan, C. Englert, M. Spannowsky, Phys. Rev. D 87 (2013) 055002, arXiv:1210.8166.
[22] J. Baglio, A. Djouadi, R. Grober, M. Muhlleitner, J. Quevillon, et al., J. High Energy Phys. 1304 (2013) 151, arXiv:1212.5581.
[23] F. Goertz, A. Papaefstathiou, L.L. Yang, J. Zurita, J. High Energy Phys. 1306 (2013) 016, arXiv:1301.3492.
[24] J. Cao, Z. Heng, L. Shang, P. Wan, J.M. Yang, J. High Energy Phys. 1304 (2013) 134, arXiv:1301.6437.
[25] R.S. Gupta, H. Rzehak, J.D. Wells, arXiv:1305.6397, 2013.
[26] D.T. Nhung, M. Muhlleitner, J. Streicher, K. Walz, arXiv:1306.3926, 2013.
[27] U. Ellwanger, J. High Energy Phys. 1308 (2013) 077, arXiv:1306.5541.
[28] D.Y. Shao, C.S. Li, H.T. Li, J. Wang, J. High Energy Phys. 1307 (2013) 169, arXiv:1301.1245.
[29] C. Han, X. Ji, L. Wu, P. Wu, J.M. Yang, arXiv:1307.3790, 2013.
[30] J.M. Butterworth, A.R. Davison, M. Rubin, G.P. Salam, Phys. Rev. Lett. 100 (2008) 242001, arXiv:0802.2470.
[31] T. Plehn, G.P. Salam, M. Spannowsky, Phys. Rev. Lett. 104 (2010) 111801, arXiv:0910.5472.
[32] C. Lester, D. Summers, Phys. Lett. B 463 (1999) 99, arXiv:hep-ph/9906349.
[33] A. Barr, C. Lester, P. Stephens, J. Phys. G 29 (2003) 2343, arXiv:hep-ph/0304226.
[34] H.-C. Cheng, Z. Han, J. High Energy Phys. 0812 (2008) 063, arXiv:0810.5178.
[35] A.J. Barr, C.G. Lester, J. Phys. G 37 (2010) 123001, arXiv:1004.2732.
[36] A. Barr, T. Khoo, P. Konar, K. Kong, C. Lester, et al., Phys. Rev. D 84 (2011) 095031, arXiv:1105.2977.
[37] A.J. Barr, C. Gwenlan, Phys. Rev. D 80 (2009) 074007, arXiv:0907.2713.
[38] G. Aad, et al., ATLAS Collaboration, Phys. Lett. B 701 (2011) 186, arXiv:1102.5290.
[39] G. Aad, et al., ATLAS Collaboration, Phys. Lett. B 710 (2012) 67, arXiv:1109.6572.
[40] G. Aad, et al., ATLAS Collaboration, Phys. Lett. B 718 (2013) 879, arXiv:1208.2884.
[41] G. Aad, et al., ATLAS Collaboration, J. High Energy Phys. 1211 (2012) 094, arXiv:1209.4186.
[42] Tech. Rep. ATL-PHYS-PUB-2013-004, CERN, Geneva, 2013.
[43] M. Cacciari, G.P. Salam, G. Soyez, J. High Energy Phys. 0804 (2008) 063, arXiv:0802.1189.
[44] M. Cacciari, G.P. Salam, G. Soyez, Eur. Phys. J. C 72 (2012) 1896, arXiv:1111.6097.
[45] K. Arnold, M. Bahr, G. Bozzi, F. Campanario, C. Englert, et al., Comput. Phys. Commun. 180 (2009) 1661, arXiv:0811.4559.
[46] T. Hahn, Comput. Phys. Commun. 140 (2001) 418, arXiv:hep-ph/0012260.
[47] T. Hahn, M. Perez-Victoria, Comput. Phys. Commun. 118 (1999) 153, arXiv:hep-ph/9807565.
[48] E. Boos, M. Dobbs, W. Giele, I. Hinchliffe, J. Huston, et al., arXiv:hep-ph/0109068, 2001.
[49] M. Bahr, S. Gieseke, M. Gigg, D. Grellscheid, K. Hamilton, et al., Eur. Phys. J. C 58 (2008) 639, arXiv:0803.0883.
[50] S. Dawson, S. Dittmaier, M. Spira, Phys. Rev. D 58 (1998) 115012, arXiv:hep-ph/9805244.
[51] D. de Florian, J. Mazzitelli, arXiv:1309.6594, 2013.
[52] T. Gleisberg, S. Hoeche, F. Krauss, M. Schonherr, S. Schumann, et al., J. High Energy Phys. 0902 (2009) 007, arXiv:0811.4622.
[53] J. Alwall, M. Herquet, F. Maltoni, O. Mattelaer, T. Stelzer, J. High Energy Phys. 1106 (2011) 128, arXiv:1106.0522.
[54] A. Denner, S. Dittmaier, S. Kallweit, S. Pozzorini, Phys. Rev. Lett. 106 (2011) 052001, arXiv:1012.3975.
[55] J.M. Campbell, R.K. Ellis, Phys. Rev. D 62 (2000) 114012, arXiv:hep-ph/0006304.
[56] J.M. Campbell, arXiv:hep-ph/0105226, 2001.
[57] J.M. Campbell, R.K. Ellis, C. Williams, J. High Energy Phys. 1107 (2011) 018, arXiv:1105.0020.

[58] S. Chatrchyan, et al., CMS Collaboration, Phys. Lett. B 713 (2012) 68, arXiv:1202.4083.
[59] G. Aad, et al., ATLAS Collaboration, J. High Energy Phys. 1209 (2012) 070, arXiv:1206.5971.
[60] A.J. Barr, S.T. French, J.A. Frost, C.G. Lester, J. High Energy Phys. 1110 (2011) 080, arXiv:1106.2322.
[61] G. Aad, et al., ATLAS Collaboration, Phys. Rev. D 84 (2011) 112006, arXiv:1108.2016.
[62] A. Elagin, P. Murat, A. Pranko, A. Safonov, Nucl. Instrum. Methods Phys. Res., Sect. A, Accel. Spectrom. Detect. Assoc. Equip. 654 (2011) 481, arXiv:1012.4686.
[63] A.W.F. Edwards, Likelihoods, Cambridge University Press, 1972.
[64] A.L. Read, J. Phys. G 28 (2002) 2693.
[65] M. Gillioz, R. Grober, C. Grojean, M. Muhlleitner, E. Salvioni, J. High Energy Phys. 1210 (2012) 004, arXiv:1206.7120.
[66] R. Grober, M. Muhlleitner, J. High Energy Phys. 1106 (2011) 020, arXiv:1012.1562.
[67] R. Contino, M. Ghezzi, M. Moretti, G. Panico, F. Piccinini, et al., J. High Energy Phys. 1208 (2012) 154, arXiv:1205.5444.
[68] W.D. Goldberger, B. Grinstein, W. Skiba, Phys. Rev. Lett. 100 (2008) 111802, arXiv:0708.1463.
[69] T. Plehn, M. Spannowsky, M. Takeuchi, J. High Energy Phys. 1105 (2011) 135, arXiv:1102.0557.